AN ABSTRACT OF THE THESIS OF

Mohammad Hashem Nehrir (Name) for the Master of Science (Degree)

in Electrical and Electronics Engineering (Major) presented on March 5, 1971 (Date)

Title: REAL-TIME PREDICTIVE VOLTAGE CONTROL OF A DIRECT-CURRENT GENERATING SYSTEM, USING A HYBRID COMPUTER

Abstract approved: Redacted for privacy

Solon A. Stone

Real-time predictive voltage control of a direct-current (d-c) generating system is achieved with the aid of a hybrid computer. Some assumptions were required to adequately simplify the simulation of the d-c generating system.

A predictive controller is used to maintain the load voltage of the d-c generating system (the controlled system) at the desired level for any change in the load. This controller consists of a fast-time scale linearized analog model of the controlled system and a control logic, which is programmed on the digital part of the hybrid computer.

In showing the applicability of the controller, the predictive control technique was first applied to the linearized analog simulation of the controlled system, and the desired control was successfully

achieved. Control of the real system was then attempted and satisfactory results were obtained.

Real-Time Predictive Voltage Control of a Direct-Current Generating System, Using a Hybrid Computer

by

Mohammad Hashem Nehrir

A THESIS

submitted to

Oregon State University

in partial fulfillment of
the requirements for the
degree of

Master of Science

June 1971

APPROVED:

Redacted for privacy

Professor of Electrical and Electronics Engineering

in charge of major

Redacted for privacy

Chairman of Department of Electrical and Electronics Engineering

Redacted for privacy

Dean of Graduate School

Date thesis is presented March 5, 1971

Typed by Barbara Eby for Mohammad Hashem Nehrir

ACKNOWLEDGEMENT

The author wishes to express sincere gratitude for the encouragement and help of Professor Solon A. Stone and Professor John F. Engle of Electrical and Electronics Engineering Department, Oregon State University. Mr. Knut Heuch deserves special plaudits for his cooperation in making this project a success. Finally, Mr. Allen Herr's valuable suggestions for the design of the current controller is genuinely appreciated.

TABLE OF CONTENTS

LIST OF FIGURES

LIST OF SYMBOLS

A = system input determined by the predictive controller

ADC = analog to digital converter

AMAX = maximum system input

AMIN = minimum system input

α = constant by which the model time constans are multiplied

C = scaled output of the d-c generating system

CD = output-rate ($\dot{c}(t)$)

CL = control line

D = error in the output (C-REF)

DAC = digital to analog converter

E = threshold limit of error

E_{ae} = exciter armature voltage

E_{ag} = generator armature voltage

E_{dc} = exciter field excitation voltage

F = threshold limit of output-rate

γ = value of C when A = 0

i_{ag} = generator armature current

i_b = base current of the transistor current controller

i_e = emitter current of the transistor current controller

i_{fe} = exciter field current

i_{fg} = generator field current

K_e = exciter gain

K_g = generator gain

L_{fe} = exciter field inductance

L_{fg} = generator field inductance

m = slope of linear response of transistor current controller

R = system input when error and error-rate are within their threshold limits

REF = reference value at which C is desired to remain

R_{ae} = exciter armature resistance

R_{ag} = generator armature resistance

R_{fe} = exciter field resistance

R_{fg} = generator field resistance

R_ℓ = load resistance

T_e = exciter time constant

T_g = generator time constant

V_b = base voltage of transistor current controller ($V_b = A$)

V_0 = generator output voltage (load voltage)

ω_e = exciter speed

ω_g = generator speed

X = coefficient of D in expression for R

Y = coefficient of CD in expression for R

REAL-TIME PREDICTIVE VOLTAGE CONTROL OF A DIRECT-CURRENT GENERATING SYSTEM, USING A HYBRID COMPUTER

I. INTRODUCTION

The first major application of the predictive control technique was presented by Chestnut in 1961 (2). In his work an on-line digital computer was used to control an aircraft landing, using the concept of predictive control. Many important applications of the predictive control have been presented since then (1, 3, 8). In nearly all the applications presented so far, a digital computer has been used. In the control problem presented in this thesis, however, a hybrid computer system is used in an attempt to gain additional speed of control.

The control system situation in hand may be described briefly as follows:

It is desired to keep the output voltage of the d-c generating system at a desired level. This was achieved by coupling the controlled system (d-c generating system) to an EAI-690 hybrid computer, on which the predictive controller was built. The predictive controller consists of a fast-time scale linear model of the controlled system and control logic. The fast model was simulated on the analog computer, and the control logic was programmed on the digital computing part of the hybrid system. The fast model is used to predict the voltage time response of the controlled system. On the basis of this predicted

response, the control logic makes the logical decisions for choosing the necessary input to the controlled system, to drive the system output to the desired level and keep it there.

A general block diagram of the control system is given in Figure 1. The components of this system will be discussed in detail, and the experimental results will be presented later in this thesis.

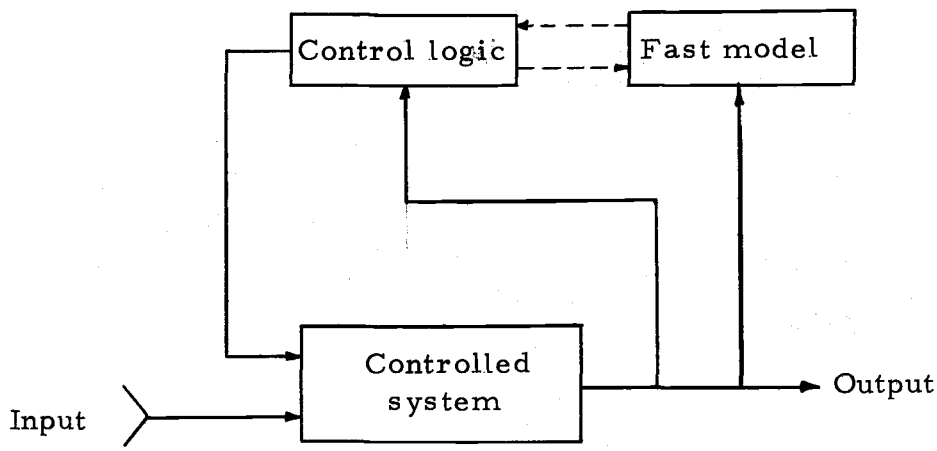

Figure 1. Control system block diagram.

II. THE CONTROLLED SYSTEM

The controlled system consists of two separately excited direct current generators whose specifications are given in Appendix C. These two generators are connected in cascade with one generator providing the field excitation for the other. This combination is shown schematically in Figure 2.

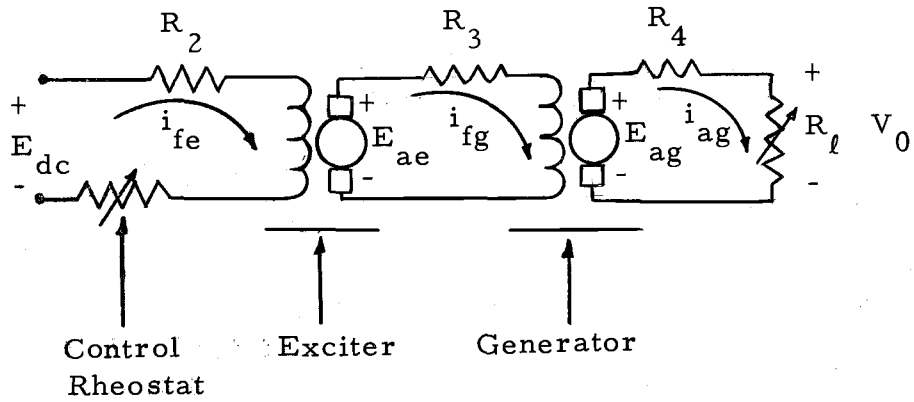

Figure 2. Schematic diagram of the d-c generating system.

When the load on the generator is varied, the load voltage V_0 varies accordingly (5). From Figure 2

$$V_0 = R_\ell i_{ag} \tag{2.1}$$

In the steady state

$$i_{ag} = \frac{E_{ag}}{R_{ag} + R_4 + R_\ell} \tag{2.2}$$

where R_{ag} is the internal armature resistance of the generator. Assuming the generator is operated within the linear region of its magnetization curve,

$$E_{ag} = K_g \omega_g i_{fg} \tag{2.3}$$

where in steady state

$$i_{fg} = \frac{E_{ae}}{R_{ae} + R_3 + R_{fg}} \tag{2.4}$$

In Equation (2.4) R_{ae} is the exciter internal armature resistance, and R_{fg} is the internal field resistance of the generator.

Similarly, the armature voltage of the exciter can be expressed in terms of its field current i_{fe}. As a result, the load voltage V_0 becomes

$$V_0 = \frac{K_e \omega_e K_g \omega_g R_\ell}{(R_{ae} + R_3 + R_{fg})(R_{ag} + R_4 + R_\ell)} i_{fe} \tag{2.5}$$

Equation (2.5) shows the linear dependency of V_0 on the exciter field current i_{fe}. Hence, a proper adjustment in the exciter field current will result in control of the load voltage V_0.

The field current control is normally accomplished by controlling the resistance of a rheostat placed in the field circuit as shown in Figure 2. In this control problem, however, a transistor current amplifier is used as the current controller. Figure 3 shows the

controlled system including the transistor field current controller. The current amplifier is designed such that the change in its output current is directly proportional to the variation in its input voltage V_b, as long as the transistor is not saturated. Hence, the exciter field current i_{fe} is properly adjusted by controlling the transistor base voltage V_b.

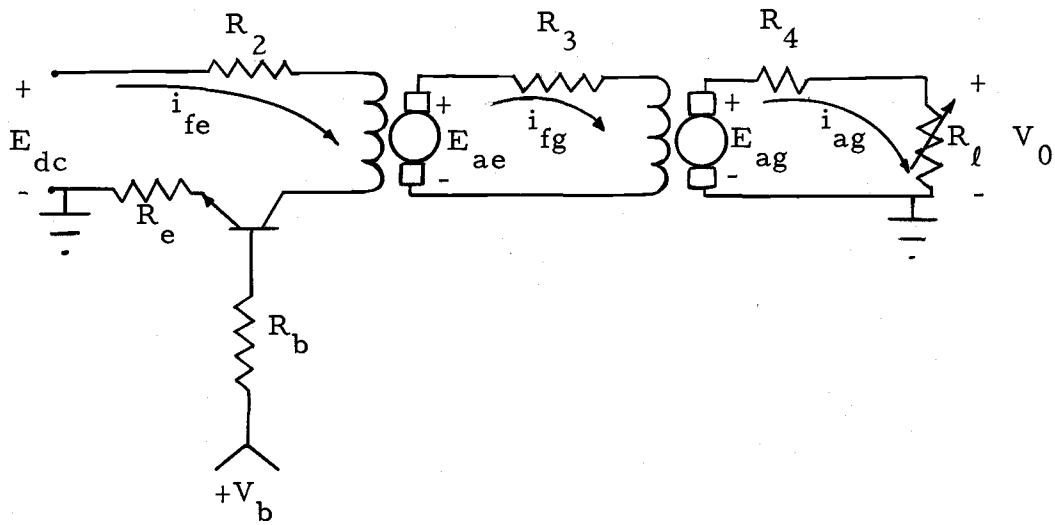

Figure 3. The controlled system including the transistor current controller.

The design procedure and specifications of the transistor current controller appear in Appendix B.

III. THE SYSTEM MODEL

Investigation of many phenomena associated with the dynamic operation of d-c machines is possible by using computer simulation techniques. Analog, digital, and hybrid computer simulations are the three simulation schemes presented thus far. The usefulness and applicability of each of the above three methods depends directly on the nature of the problem.

In the present control problem a linear analog model of the controlled system is used. This is a sufficient model for the predictive control technique used herein, because

1. The generators are operated within the linear region of their magnetization curve.
2. In predictive control, an accurate model of the controlled system is not necessary (1).
3. The fast time response of the system model is of prime importance, and the fast-time scale analog simulation of the system has this property.

The particular simulation described herein is for the system shown schematically in Figure 2, with both the exciter and generator subject only to field control, and operating at constant speed.

Since the generators are assumed to operate within the linear region of their magnetization curves, the ordinary linear differential

equations describing the linear characteristics of the machines are applicable. This linear property will be used to express the relationship between the output and the input voltage of each generator in the form of a transfer function. From Figure 2

$$E_{dc}(t) = (R_2+R_{fe})i_{fe}(t) + L_{fe}\frac{di_{fe}(t)}{dt} \qquad (3.1)$$

and

$$E_{ae}(t) = K_e \omega_e i_{fe}(t) \qquad (3.2)$$

where R_{fe} and L_{fe} are the internal resistance and inductance of the exciter field winding. Assuming zero initial conditions and taking the Laplace transform of Equation (3.1) and (3.2), Equations (3.3) and (3.4) will result respectively.

$$E_{dc}(s) = (R_2+R_{fe}+sL_{fe})I_{fe}(s) \qquad (3.3)$$

$$E_{ae}(s) = K_e \omega_e I_{fe}(s) \qquad (3.4)$$

Finally, the transfer function will result by eliminating $I_{fe}(s)$ from Equations (3.3) and (3.4), as given in Equation (3.5).

$$\frac{E_{ae}(s)}{E_{dc}(s)} = \frac{K_e \omega_e}{(R_2+R_{fe})(1+sTe)} \qquad (3.5)$$

where K_e is the exciter gain, ω_e is the speed of rotation of the

exciter, and $Te = \frac{L_{fe}}{R_{fe} + R_2}$ is the time constant of the exciter field winding.[1]

Because of the neglected effect of armature inductance and resistance, the time response of the armature voltage of the exciter is the same as the field excitation signal for the generator. Using the same technique used above, the transfer function describing the ratio of the output and input voltages of the generator will be:

$$\frac{E_{ag}(s)}{E_{ae}(s)} = \frac{K_g \omega_g}{(R_{fg} + R_3)(1 + sT_g)} \qquad (3.6)$$

where K_g and ω_g are respectively the gain and speed of rotation of the generator, and

$$T_g = \frac{L_{fg}}{R_{fg} + R_3}$$

is the time constant of the generator field winding.

Product of Equations (3.5) and (3.6) will give the over-all transfer function of the controlled system as follows:

$$\frac{E_{ag}(s)}{E_{dc}(s)} = \frac{K}{(1 + sT_e)(1 + sT_g)} \qquad (3.7)$$

---

[1] Resistors R_2 and R_3 are used in series with the field winding of the exciter and generator, respectively, for current limiting.

where

$$K = \frac{K_e K_g \omega_e \omega_g}{(R_{fe} + R_2)(R_{fg} + R_3)}$$

is the over-all system gain.

The basic analog simulation of the controlled system will result from Equation (3.7). The analog flow diagram for this simulation is shown in Figure 4. Equation (3.7) and Figure 4 show that the controlled system is modeled as a linear, second order system.

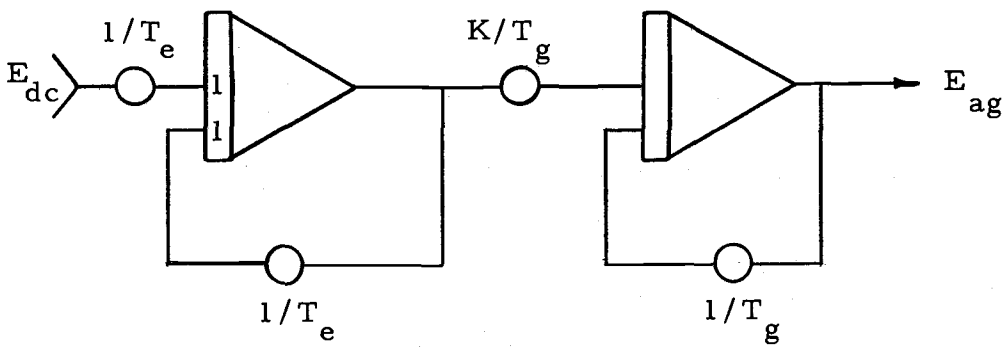

Figure 4. Basic analog simulation flow diagram.

To obtain the fast-time scale analog model of the controlled system, the gain of the integrators in Figure 4 are increased by factor of 10 or 100 as desired, to make the model 10 or 100 times faster. The initial conditions on the integrators of the fast model, while being used in connection with the controlled system, are functions of the current state of the system. The detailed analog flow diagrams of the

fast-time scale model, used in connection with the simulated controlled system and the real-time system, are given in Appendix D.

IV. THE PREDICTIVE CONTROLLER

The basic principle of any predictive control technique is the use of the fast-time simulation of the controlled system and the control logic. The fast-time model is obtained by reducing the system time constants by some factor (typically 100 or 1000). The control logic is used to determine the input signal level to the controlled system and the fast model.

From Pontryagin's Maximum Principle (7) it may be shown that for time optimal control of such systems, the input must always take an extreme value at either its higher or lower limit. Since for time optimal control the system has a bang-bang input, the input to the fast model will also be bang-bang, and the purpose of the controller is to answer the question, "In which direction must full system drive be applied?" The control logic will then determine the level and duration of the input signal to the controlled system.

The response of the predictive controller depends directly upon the location of the controlled system response in the error, error-rate phase-plane.[2] When the system phase-plane trajectory starts in the first or third quadrant, or is extended to these regions, the system is going away from synchronization (zero error in the system output response). No prediction is necessary in these two regions,

---

[2] Error = output response, C , less the desired reference.

as the direction to drive the system is obvious, and the input level is chosen to dirve the system in such direction. This input will drive the trajectory from the first or third quadrant to the fourth or second quadrant, respectively, as presented in Figure 5. As soon as the trajectory enters the second or fourth quadrant, the prediction process begins, in order to determine the correct system input switching time. Up to this point, the model has been in "initial condition". At the start of the prediction process, the model is set to the present state of the system. It is then allowed to run under the input level opposite to that of the system input. The model predicts the system response under such input, and continues to run until the predicted error-rate reaches zero. At this time the model goes into "hold", and the predicted error is computed and compared with the present value of the actual system error. If at this moment the predicted error has the same polarity as the actual system error, the model is reset to the present state of the system, and prediction process continues until such time that the predicted error becomes zero or changes polarity. At this time, the system input switches level to bring the system toward synchronization. The predicted trajectories are shown dotted in Figure 5. In this figure three different cases are shown. In case a, the trajectory starts in the third quadrant and is driven into the second quadrant, where repetative predictions are made in order to find the correct

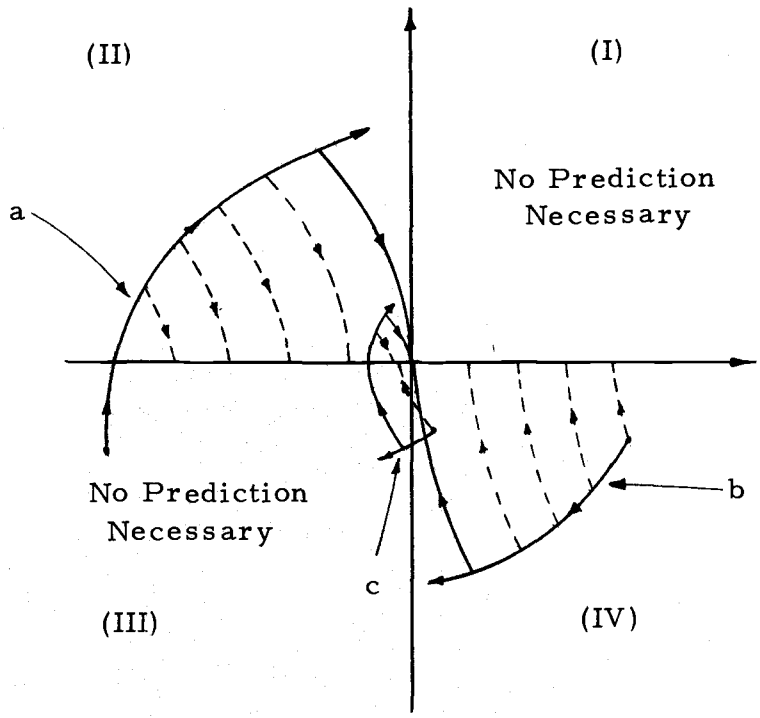

Figure 5. Error, error-rate phase-plane portrait, showing different trajectories.

time to switch the system input level. In case b, the trajectory begins in the fourth quadrant, and the prediction process starts immediately. In case c, the trajectory starts in the fourth quadrant, but the first prediction makes the predicted error negative, while the present system error is still positive. Thus, the system input switches level immediately. Under the new input, the system trajectory is driven into the third and then to the second quadrant, where the prediction process starts again. Finally, the input level is switched, and the system is brought to rest at zero error, under the influence of this input.

Now, consider the error, error-rate phase-plane portrait for a predictively controlled system, given in Figure 6. At starting point a , the system is loaded such that the output is less than the chosen reference and decreasing, thus both error and error-rate are negative. Hence, the system input is kept at its upper level to make the system go toward synchronization. No prediction is necessary, so long as the error and error-rate have the same polarity, as the direction the system is to be driven is obvious. Prediction begins when the error-rate becomes positive. At point b the first prediction is made to observe the predicted error when the predicted error-rate reaches zero. Successive predictions are made until finally the predicted error changes polarity when the error-rate becomes zero at the origin. Since the predicted error has reached zero, it is time for the system input level to switch, and the control logic operates to perform such switching.

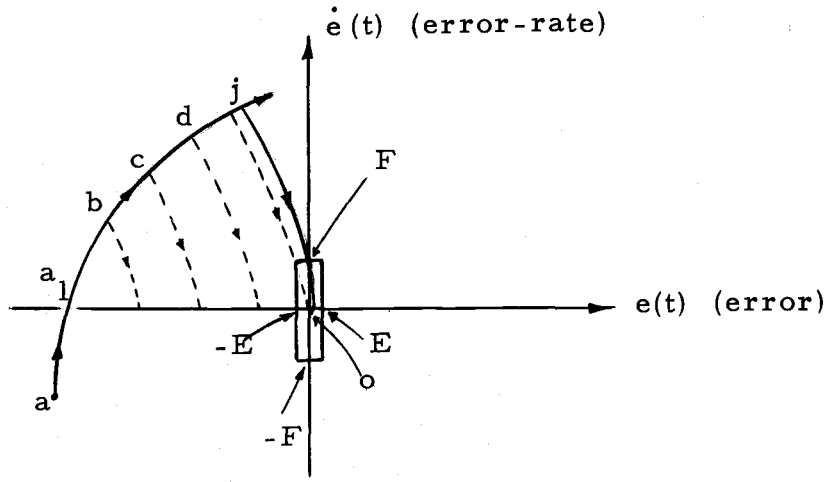

Figure 6. Error, error-rate phase-plane portrait of the predictive controller.

In order to prevent any undesired overshoot, the input switching can occur at a slightly earlier time, so that the real-time phase-plane trajectory will directly hit the origin without any overshoot. This is accomplished by making the model time constants larger than their corresponding system time constants (8). The factor by which the system time constants are to be multiplied to result the time constants of the model, can best be determined by trial and error. This factor is a function of the prediction rate and the existing time delay in transfer of information between the analog and digital computers in use.

Beyond point o there exists a limit cycle about the origin. The magnitude and frequency of this limit cycle depend in large part upon the prediction repetition rate. Because this rate is relatively high, the magnitude of oscillation can be small and the frequency high depending on the nature of the controlled system and the speed of the control logic that performs the switching functions. Sophistication of the control logic provides a mean for reducing the magnitude of the limit cycle. This magnitude is reduced appreciably by reducing the amplitude of the system input, when the present error and error-rate are less than certain threshold values (2). This reduction in the amplitude of the system input is made by making the input a function of the present values of the error and error-rate, when these two variables are within their threshold values, E and F , respectively. In this linear region bonded by E and F, as shown in Figure 6, the

input is computed as follows:

$$R = XD + Y\ CD \qquad (4.1)$$

The parameters X and Y, and also E and F are constants, and a part of the computer program input parameters.

The real-time phase plane trajectory starts from point a in Figure 6 and passes through points b, c, d, j, and o. Along this trajectory, time takes on real-time dimensions. The predicted trajectories, shown dotted in Figure 6, are obtained from the fast-time scale model and along these trajectories time takes on computer time dimensions.

In achieving the predictive controller, discussed above, the fast time scale linear model of the controlled system was simulated on the analog computer (EAI-680), as discussed in part III of this thesis. The logical decisions were made using the EAI-640 digital computer. These two computers were connected to make the EAI-690 hybrid computing system.

The details of how the logical decisions are made will be clearer after discussing the "control logic" part of the predictive controller.

Control Logic

The heart of the predictive controller is the logic section. In its simplest form the control logic is just a means of mechanizing the

switching criteria that were introduced in the preceding section. This procedure is summarized in a computer flow-chart, as shown in Figure 7. From the chart it can be seen that after the input parameters are accepted and the depended parameter, AMED defined, the first step is to compute the present values of the error D , and the error-rate CD . Note that the error-rate and the output-rate are equivalent since the error and the output differ only by a constant, REF . To obtain the output-rate CD from the output C , the analog differentiation technique was used. Design and specifications of the differentiator appear in Appendix A.

At the beginning of each cycle the absolute values of D and CD are compared with their respective threshold values, E and F. If both of the absolute values are within their threshold limits, Equation (4.1) determines the proper input to the controlled system. If either or both, D and CD , are not within their threshold values, their polarities are compared. If D and CD have the same polarity, the controlled variable C is moving away from synchronization, and the system input is chosen to drive the system toward synchronization, as quickly as possible. The choice of the input level is apparent so that no prediction is necessary. An example of this condition would be segment aa_1 in Figure 6. When the error-rate changes polarity under the influence of the new input A , the controlled variable C , is moving toward synchronization, and if the input signal is switched at

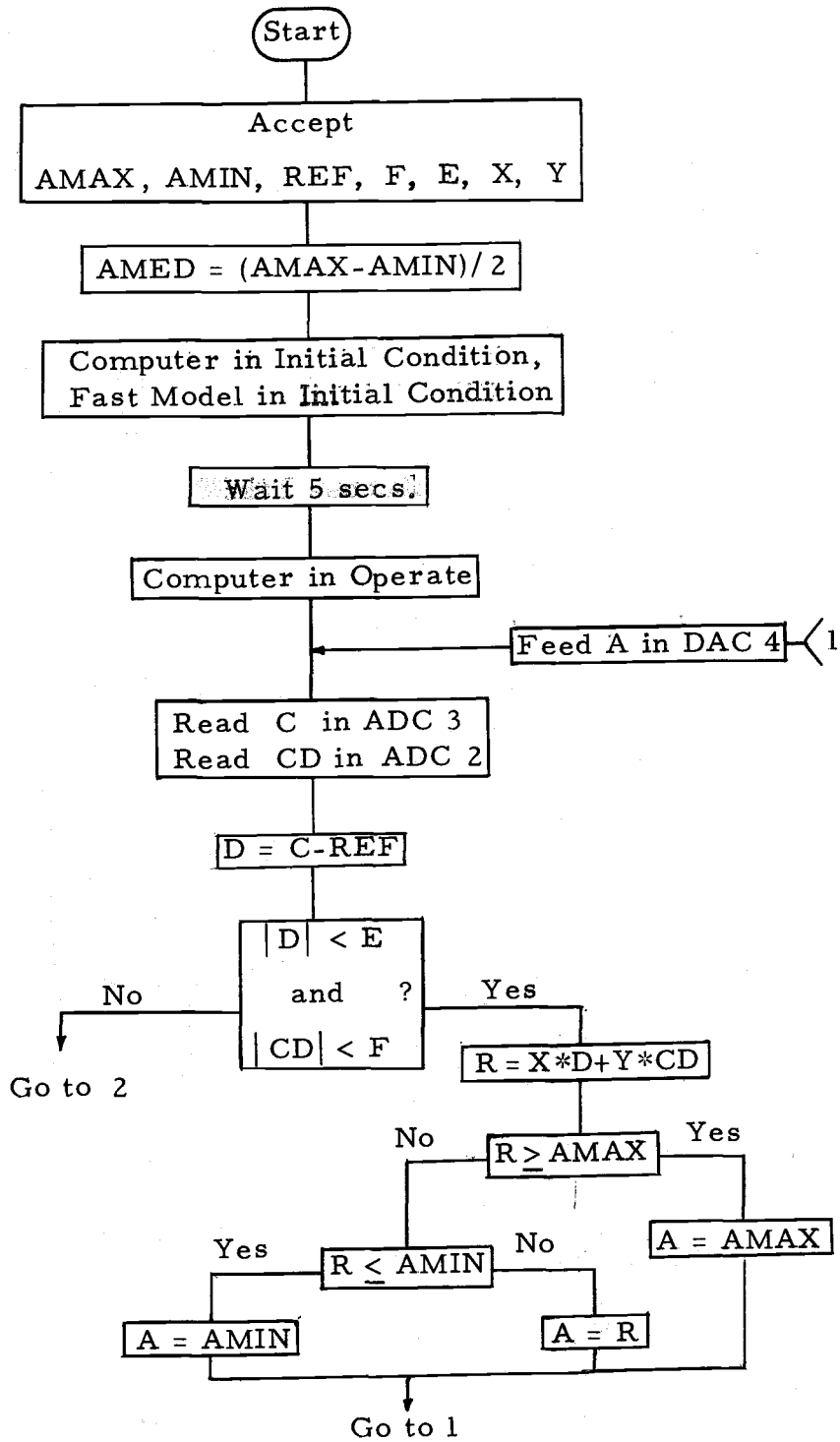

Figure 7. The control logic computer flow chart.
(Figure 7 is continued on the next page.)

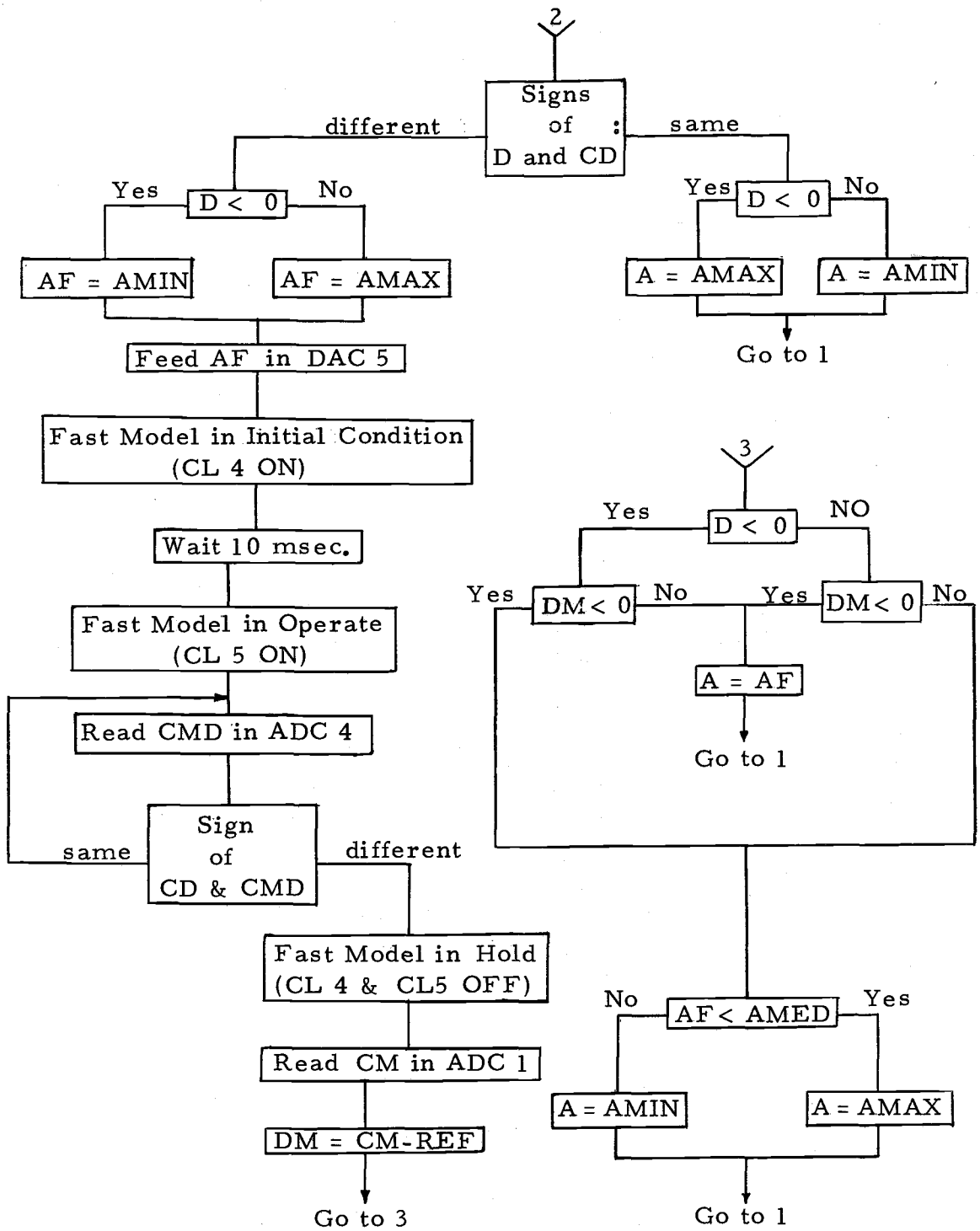

Figure 7 continued.

precisely the right time, a deadbeat response will result. Thus the predictive system logic calls for repetative computations to determine whether future synchronization would occur if the input to the controlled system were switched to its other limit at the present instant of time. For this purpose the fast-time scale model operates to determine the future response of the system under the given input. When the predicted error-rate reaches zero at the end of each computation, the model goes into "hold" and the polarity of the predicted error is checked against the polarity of the actual system error. As a result, the inputs to the model and the controlled system are determined as explained in the preceding section. Finally, when the predicted error reaches zero or changes polarity, the control logic calls for a switching in the controlled system input, which drives the system toward synchronization.

The prediction and switching processes are shown in Figure 6. In this figure predictions are made for trial switchings from point b through j. When the response reaches point j, the logic indicates future synchronization will occur if the input is switched immediately. Finally, it may be seen that synchronization does occur at the origin, where both error and error-rate reach zero. Note that prediction continues until the trajectory in Figure 6 enters the dead band region, made by the threshold values E and F. In this region the system is driven toward synchronization, through a linear control of the system

input A , as given by Equation (4. 1).

It can be noticed from the computer flow chart that the system fast-time scale model stays in the operating mode only when predictions are taking place. Before the model goes into operating mode, it stays in initial condition for a very short time (10 milliseconds), to prevent any transient signals from affecting the operation.

The system input A , which is a voltage determined by the predictive controller, controls the output C through a feedback adapter. This adapter is a transistor current controller whose output current is a function of its input voltage A .[3] Finally, the exciter field current is affected by the output current of the current controller, through which the control of the output variable C is resulted. Design of the current controller is presented in Appendix B.

Figure 7 shows the flow chart for the control logic part of the predictive controller. The controlling variable A , determined by the predictive controller, was directly fed into the controlled system, and the desired control of the output, C , was achieved. Figure 8 shows a detailed block diagram of the entire system, showing all the components discussed thus far.

---

[3] $A = V_b$.

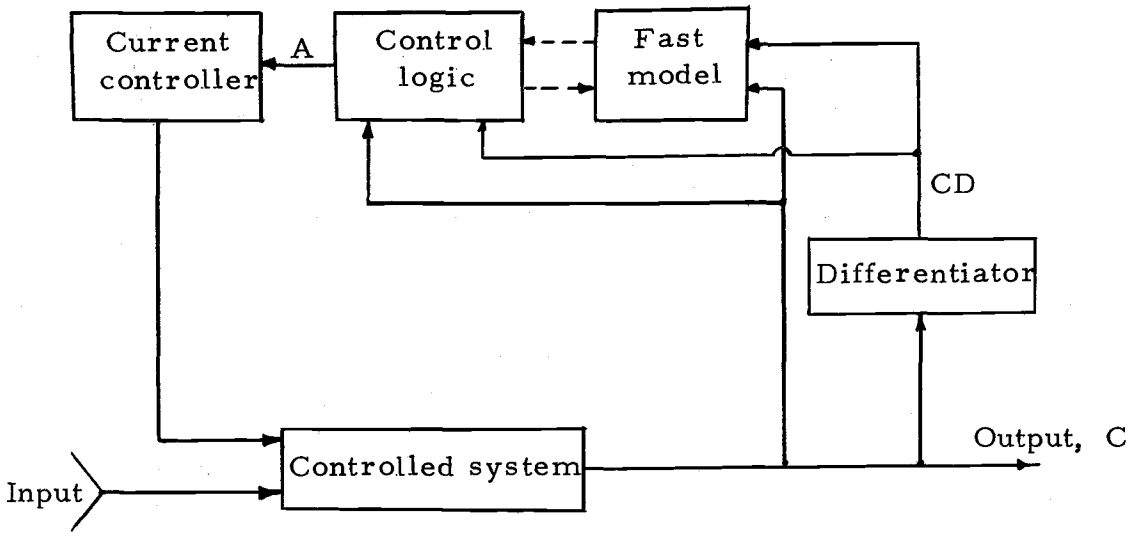

Figure 8. A detailed system block diagram.

V. THE DATA CATALOG

Introduction

The data presented herein have been selected to show the applicability of predictive control technique to the control problem previously discussed. The general aim has been to provide a qualitative analysis of the data, in addition to pointing out the conditions under which each set of data has been taken.

In order to assure the applicability of the predictive control technique to a real system, the controlled system was first simulated on the analog computer, to which the predictive control technique was applied. After this control was achieved successfully, control of the real-time system was considered. The data obtained from the control of the simulated and the real-time systems will be presented and discussed in this chapter.

Presentation of Data

Results of Simulation

A linearized model of the generators was simulated on the analog computer, as discussed in part III, to represent the real-time system. The fast time scale model used in the predictive controller was simulated similarly. The only difference between the two models is that

the gain of the integrators in the fast model are 10 times higher than the gain of the integrators used in the model representing the controlled system. This allows the time response of the fast model to be 10 times faster than the time response of the model representing the real time system. Also, the time constants of the fast model were chosen 1.8 times higher than the actual system time constants. This was done to prevent the slight time delay in the switching time of the system input A, when the error and the error-rate reach zero (8). The factor 1.8 was chosen by trial and error, and it seemed to give the correct switching time for a satisfactory control.

The controlled system and the fast model were simulated on the EAI-680 analog computer and the control logic part of the control system was programmed in assembly language on the EAI-640 digital computer. The analog simulation diagram of the controlled system in connection with the fast model is given in Appendix D, Figure D-1. The computer flow chart of the control logic appears in Figure 7. The simulated control system was disturbed by positive and negative step signals, which correspond, respectively, to sudden decrease and sudden increase in the load of the d-c generating system. The disturbance was a step input signal suddenly applied to the simulated controlled system, through the electronic switch S_1 (see Figure D-1, Appendix D).

It was arbitrarily chosen that under any load conditions the system output, C , be controlled to a constant reference value of 5 volts. The results of this control appear in Figure 9. The curves in Figure 9-a show the system response when a positive disturbance is applied to the system. Figure 9-b shows the system response when a negative disturbance is applied. Note that in the system response shown in Figures $9\text{-}a_2$ and $9\text{-}b_2$, the polarity of the disturbance is different as well as the magnitude of the disturbance, but in both cases the output C is controlled to the desired level.

In Figure 9-a, when the positive disturbance is applied to the system, the system output (Figure $9\text{-}a_2$) stays above the reference, which makes the error positive. The system input A , (Figure $9\text{-}a_1$), therefore stays at its lower level to make the system output, C , go toward the reference. Since the error is positive and decreasing, the error-rate is negative. Hence, the error and error-rate have different polarities, and the predictive controller starts predicting the future value of A, necessary to bring the system output, C , to its desired level. The predictions are clear from Figures $9\text{-}a_4$ and $9\text{-}a_5$. Everytime the model output-rate reaches zero, the model output is compared with the chosen reference, until the model output reaches the reference. At this time the control logic calls for system input switching, and the input tends to switch to its upper extreme. However, in this case by the time the input switching occurs, the error

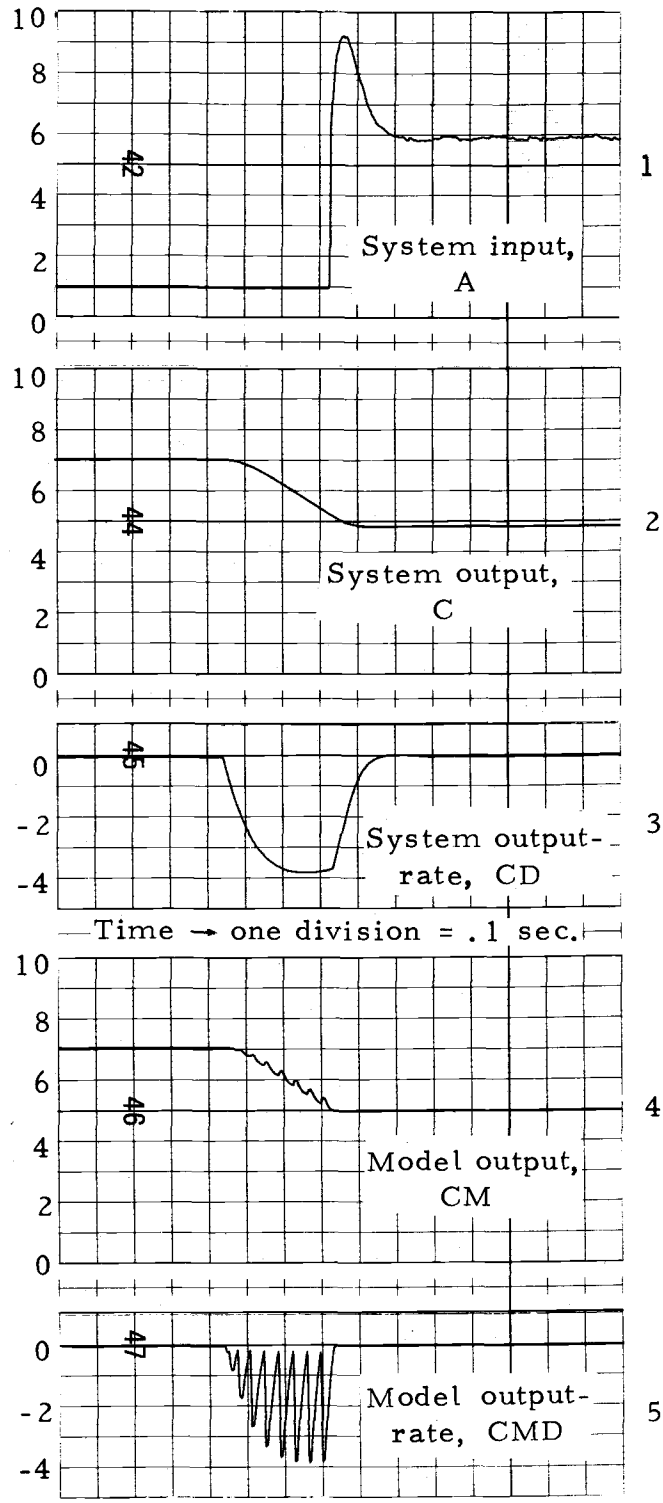

a. positive disturbance

Figure 9. Response of the control system simulation when disturbance is applied.

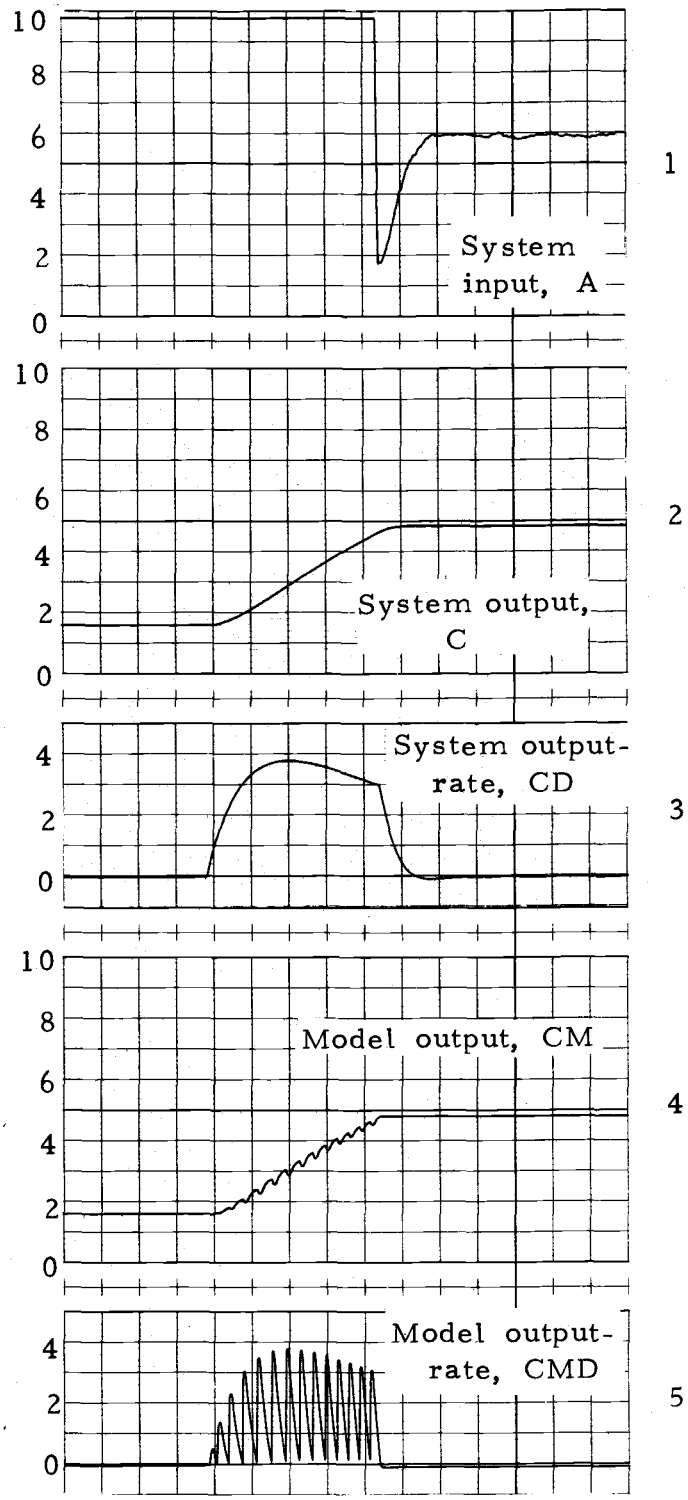

Vertical Scales are in Volts

b. negative disturbance

Figure 9 continued.

and error-rate are within their threshold limits, (discussed in part IV), and the input A becomes a linear combination of the error and error-rate (Figures 9-a_1 and 9-b_1).

In Figure 9-b when the negative disturbance is applied, the output stays below the reference, which makes the error negative. Input A therefore stays at its upper limit to force the system output to the reference level. Since the error is negative and increasing, the error-rate is positive, and the prediction process starts to determine the input switching time. Curves of Figure 9-b show the result of this control.

It is clear from Figures 9-a_2 and 9-b_2 that in both cases the output C is controlled to its desired level (5 volts). A 4% steady state error exists in the controlled output because of the fact that in reality the error D can never be zero, in steady state. The steady state value of the input A is only a function of the error, since in steady state the time-rate of the error is zero. Hence, if the error reaches zero in steady state, input A vanishes, and the system output can not remain at its desired level. From Equation (4.1) it is clear that the amount of steady state error is a function of X.

The noise existing in the steady state input is a part of the steady state value of the output-rate CD. Although, in this case the external analog differentiator is not used, and the time derivative of the output is obtained directly from the analog simulation of the system,

still some noise exists in the steady state input, because of the extremely low steady state value of the output-rate.

The input parameters of the computer program used in obtaining the results shown in Figure 9 are as follows:

AMAX = 9.8 volts	E = 0.25 volt
AMIN = 1.0 volts	X = - 8.85
REF = 5.0 volts	Y = - 0.625
F = 3.8 volts/sec.	

Results of Control of the Real System

Control of the d-c generating system was achieved by applying the previously discussed control technique to the system. The schematic diagram of the controlled system in connection with its fast time scale analog model is given in Appendix D. Figure D-2, and the computer flow chart for the control logic part of the controller is given in Figure 7. Three different sets of data were obtained under different load conditions to assure the applicability of the control technique, even in the worst cases of load variation. These three cases will be considered below and experimental results will be shown.

1. Steady increase or steady decrease in the system load.

The first observation was obtained when the load, R_ℓ, was steadily increased and decreased at a relatively constant rate. Because of the fast response of the controller, the controlled output C stayed

steadily at the chosen reference, without any fluctuations. Figure 10 shows the results of this control. Since the error, (C-REF), and the error-rate are within their threshold limits while the load is increasing (or decreasing), Equation (4.1), (A = R = XD + Y CD) determines the system input, A.[4] Hence, when the load is increasing, the load voltage decreases, and as a result, error D decreases with the same rate. But, since X is a negative number, the system input, A = R,

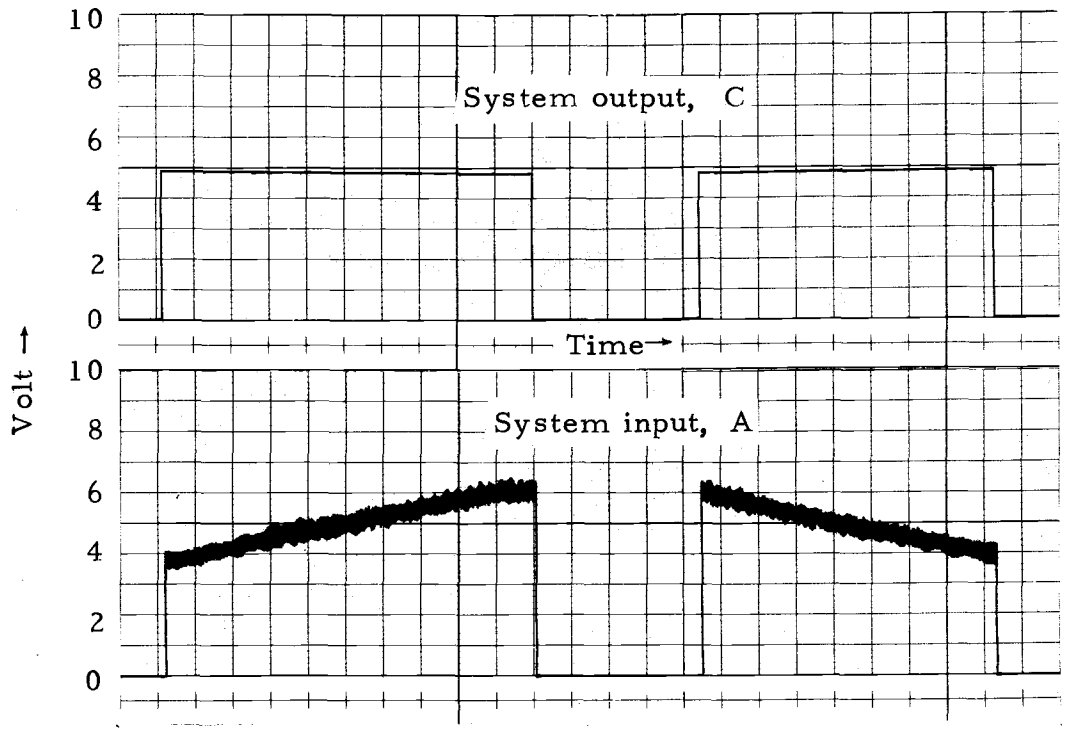

a. load increasing b. load decreasing

Figure 10. Response of the controlled system to the steadily increasing and steadily decreasing loads.

[4] Note that A and V_b are the same. A is the analog notation for the input signal to the transistor current controller.

increases with the necessary rate to keep the controlled variable at its desired level. On the other hand, when the load decreases, the load voltage goes up and the controller calls for the necessary decrease in the input signal, A , to keep the load voltage at the chosen reference. Figure 10-a shows the system output C , and the system input A , when the load is steadily increasing, and Figure 10-b shows the same two parameters for a steadily decreasing load.[5] The system output stayed at the arbitrarily chosen reference, (in this case 5 volts), throughout the loading and unloading processes. A relatively negligible steady state error exists in the controlled output, whose cause was discussed in the previous section of this chapter.

2. Sudden loading and sudden unloading of the system.

The worst case of load variations is when the system is loaded to its full capacity from the no-load state, or vice versa. Control of the system was therefore achieved under the two above mentioned load variations to assure the applicability of the control technique and control of the system under any other types of load variation. Figure 11 shows the results obtained for control of the load voltage when the system suddenly went from no-load to full-load state (Figure 11-a) and when the system went to no-load condition from the full-load state (Figure 11-b).

---

[5] The cause of existance of noise in the input signal, A , will be explained later in this chapter.

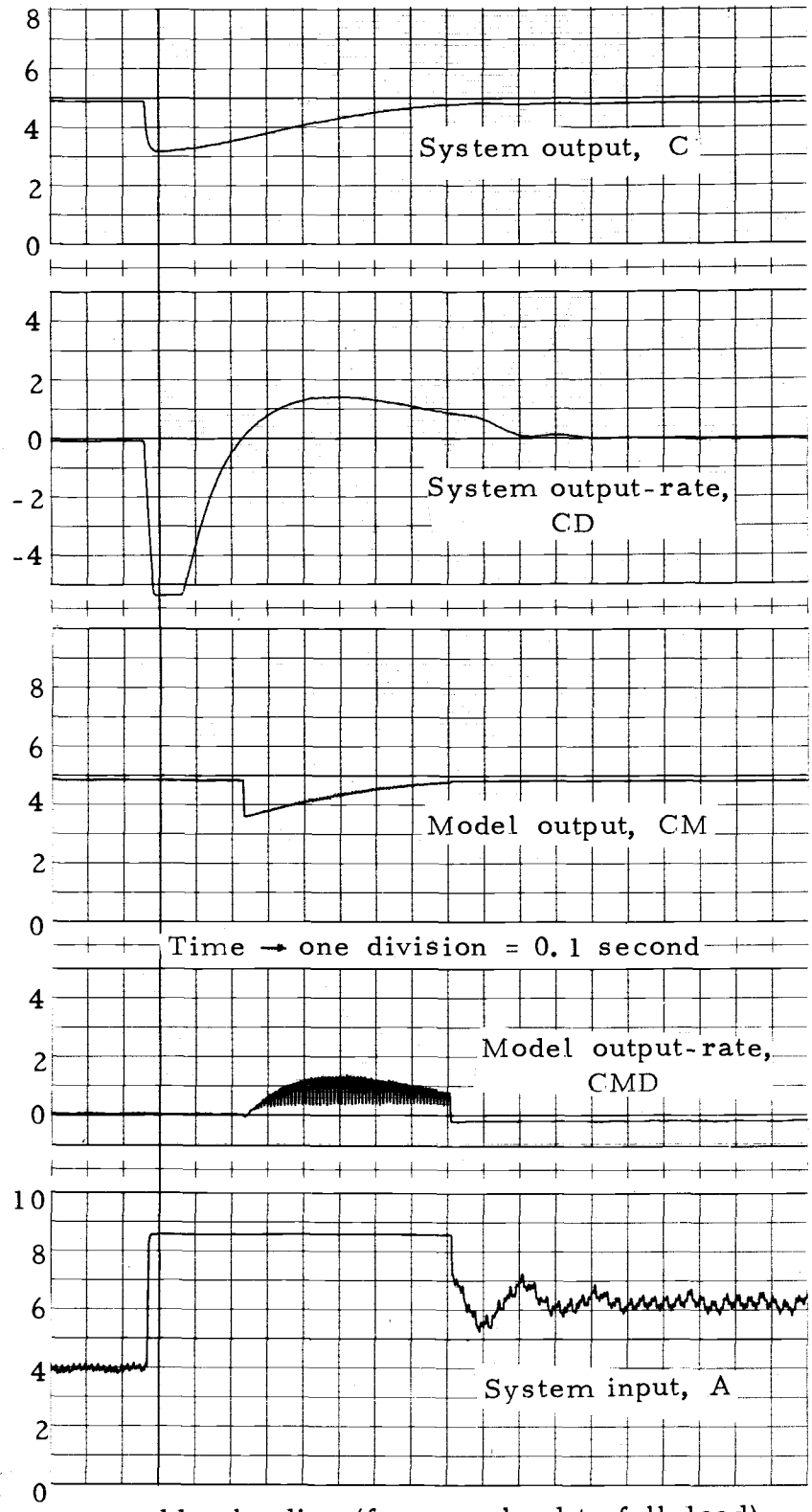

a. sudden loading (from no-load to full-load)

Figure 11. System response for sudden loading and sudden unloading.

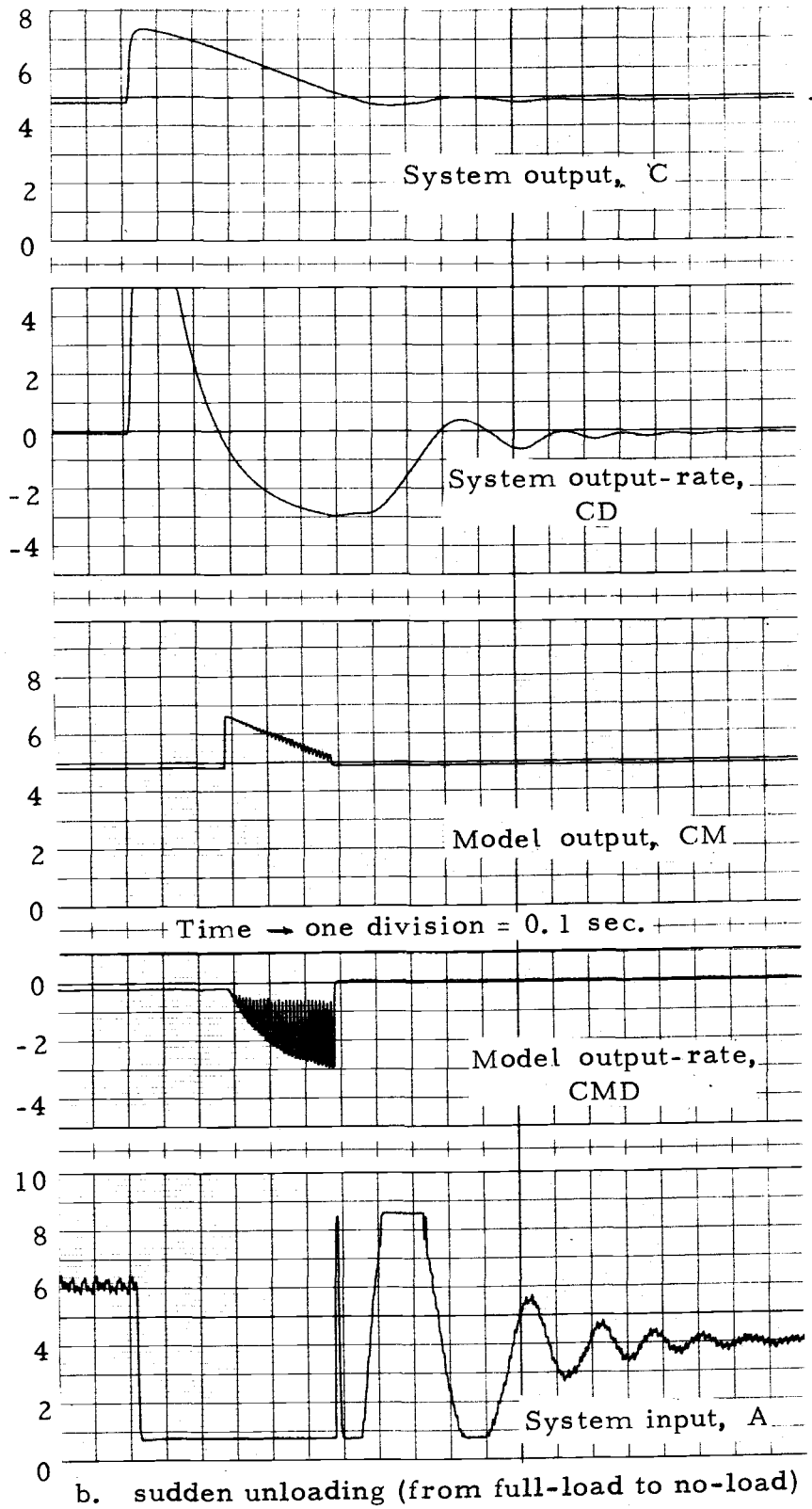

Vertical Scales are in Volts

b. sudden unloading (from full-load to no-load)

Figure 11 continued.

In the response shown in Figure 11-a, the system at the start is in the no-load condition. As soon as the system is suddenly loaded to its full capcity, the load voltage V_0 (the system output C) goes below the reference, making the error and the error-rate negative. In this state the phase plane trajectory is in the third quadrant of the phase plane. The controller therefore sets the system input at its highest level to drive the system toward synchronization. Immediately after the error-rate (output rate) changes polarity the controller calls for repetative predictions to determine the correct input switching time, at which the input is switched in order to drive the system output toward the arbitrarily chosen reference, (5 volts). In this case, however, when the input switching occurs, the error and error-rate are within their threshold limits and the linear control, (A = R = X D + Y CD), is applied to the system to bring the output to its desired reference. In the response shown in Figure 11-b, on the other hand, the system at first is fully loaded. As soon as the system is suddenly unloaded, the output tends to raise, making the error and the error-rate positive. The input, therefore, stays at its lower limit to drive the output toward the reference. When the error-rate changes polarity, the repetative prediction process begins, and the correct input switching time is determined. After switching, the input stays at its upper level for a short time before the error and error-rate go within their threshold limits. From here on, the linear control of the input

(A = R = XD + Y CD) will drive the system output, C , to the desired level (5 volts).

3. A sudden disturbance in the input to the current controller.

The last set of data was taken for control of the generating system when the input to the current controller, (V_b = A), was disconnected for a short period of time. The results of this control is shown in Figure 12. The system was loaded, and the controller operating to keep the system output at the desired level. At time t_1 (Figure 12-e) the input to the current controller was disconnected, and remained disconnected until time t_2. During this time the exciter field current is nearly zero, and the output drops down to some small value.[6] As soon as the system input is reconnected, at time t_2, the input jumps to its upper limit to drive the system output to the reference, by maximum effort. The correct input switching time, t_3, is determined by the controller, through the repetative predictions. Finally, after the error and error-rate become small enough that both are within their threshold limits, the system output is controlled to the reference through the linear control of the system input, (A = XD + Y CD).

The error, error-rate phase-plane portrait was also obtained when the system input was suddenly dropped to zero for a short

---

[6] From Figure B-2, (Appendix B), C is approximately one volt when A = 0 .

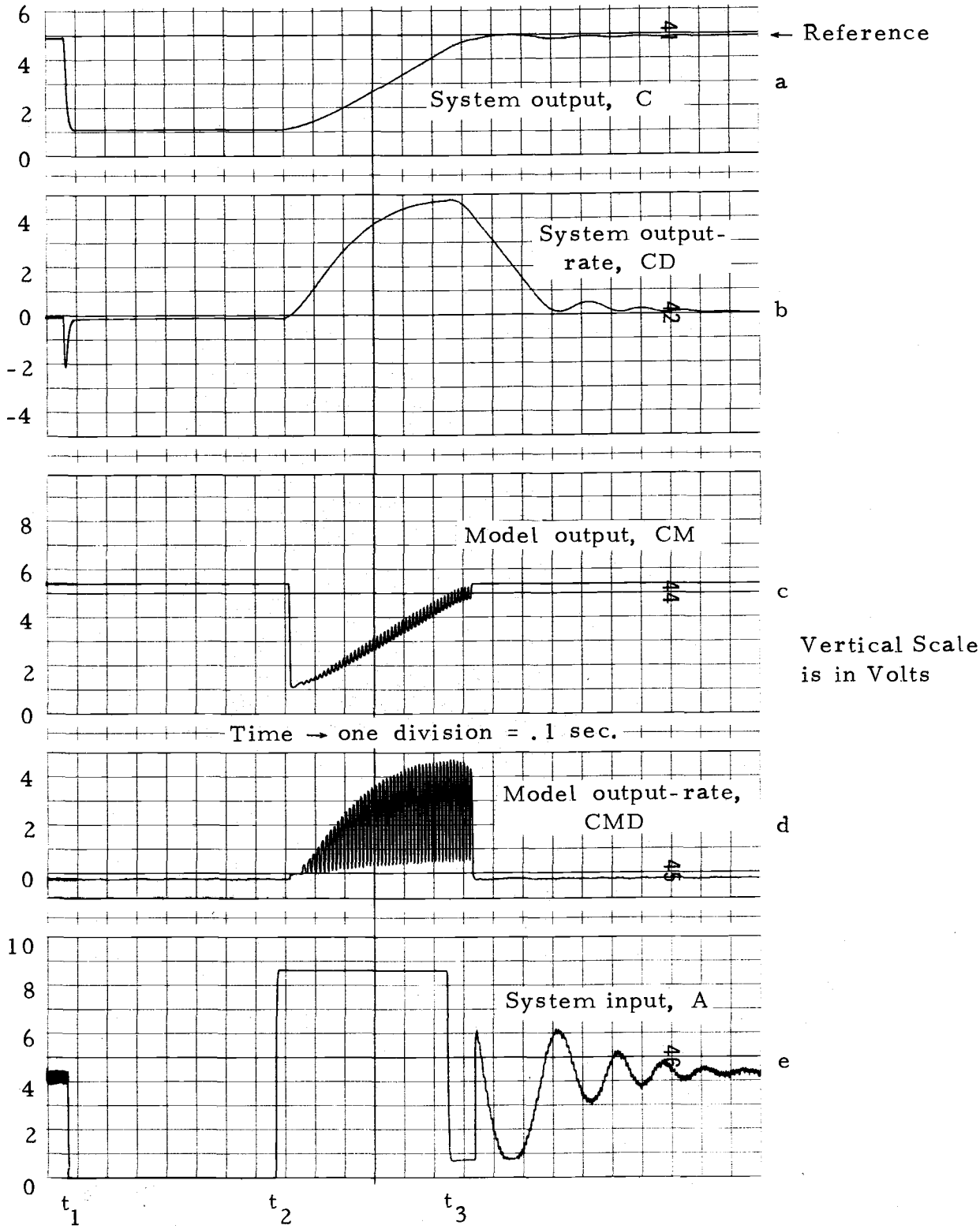

Figure 12. System response when the input to the current controller is disconnected for a short period of time.

period of time. This was done for the sake of comparison between the experimentally observed, and the theoretically developed phase-plane portraits. The theoretically developed phase-plane was shown in Figure 6, with the solid line showing the real-time trajectory. This trajectory is comparable with the experimentally obtained phase-plane trajectory shown in Figure 13. The phase-plane was observed on the oscilloscope at the same time the results shown in Figure 12 were obtained, and a picture was taken. Figure 13 shows a trace of the picture. Instants t_1, t_2, and t_3 in Figure 13 respectively correspond to t_1, t_2, and t_3 in Figure 12.

The experimental results presented in this section were obtained with the following conditions on the fast time scale model.

The model time response was 100 times faster than the system time response, the model time constants were 10 times their corresponding system time constants, and the input parameters of the computer program were as follows:

AMAX = 8.6 volts	F = 8.6 volts/sec.
AMIN = 0.8 volt	X = - 5
REF = 5 volts	Y = - 0.1
E = 0.2 volt	

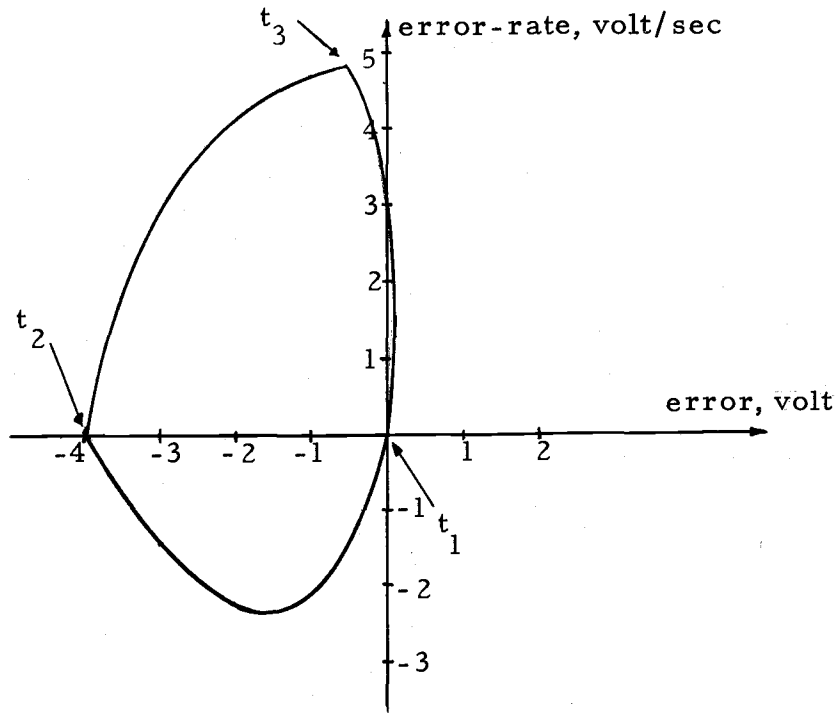

Figure 13. Error, error-rate phase-plane portrait corresponding to results of Figure 12.

General Comments

There are two important points worthwhile mentioning about the experimental results presented in this chapter. The first point is that in the analytic development of the predictive controller, it was noticed that the model output-rate reaches zero at the end of each prediction. However, this is not true for the model output-rate curves given in Figures 11 and 12. But, this is only because of the disability of the strip chart recorder pens, with which the data was recorded, to respond to the high prediction repetition rate of the predictive controller. To prove this, a picture of the model output-rate was taken

when the system input was suddenly dropped to zero for a short period of time, The picture, shown in Figure 14, was taken when the model output-rate was displayed on an oscilloscope. From this figure it is clear that the model output-rate is at zero at the end of each prediction.

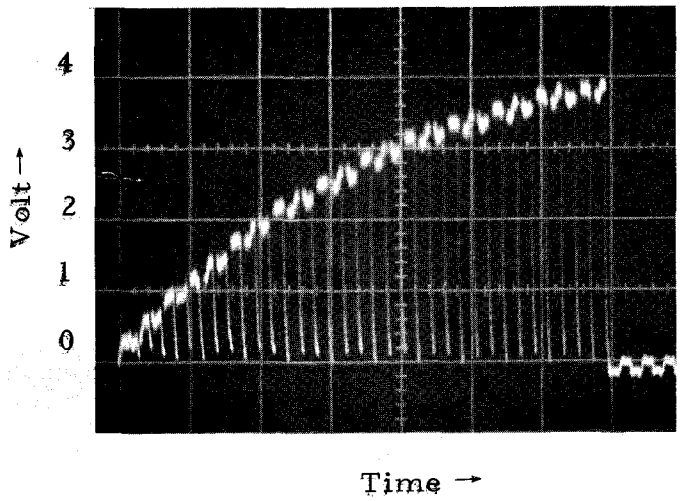

Figure 14. A picture of the model output-rate, showing the repetative prediction process.

The second point to be noticed in Figures 10 through 12 is the source of noise existing in the system input signal, A . A considerable amount of noise was generated in the system input, and system output because of the improper grounding in the previously built transmission lines which coupled the d-c generating system and the EAI-690 hybrid computer. Most of the high frequency noise was suppressed by using low pass filters and analog noise eliminators, at

both ends of the coupling transmission lines. Even though the noise suppressor did not eliminate all of the undesired noise, it eliminated enough to make the system output response noise free. The remaining noise in the system input (in Figures 10, 11, 12), which is only a small portion of the total noise, was not eliminated by the noise suppressor. The combination of the filter and the analog noise eliminator, is shown as the noise suppressor in the schematic diagram of Figure D-2, Appendix D.

VI. CONCLUSIONS

Voltage control of a d-c generating system has been achieved with the aid of a predictive controller, using a hybrid computer. Successful use of this controller in providing sufficiently high speed of control shows the advantage of on-line, hybrid computer control of the d-c generating system.

The following important conclusions are drawn from the predictive voltage control of the d-c generating system.

1. An accurate fast-time scale model of the controlled system is not necessary for sufficient performance of the predictive controller.
2. Additional speed of control is obtained by making the system input, A , take an extreme value at either its highest or lowest limit, when possible.
3. The amount of overshoot in the controlled output is a function of the model time constants, and the speed of response of system model.

It is noticed that the exciter time constant and the total system gain will change when the system load and/or the system input, A , vary. These facts have not been considered in making the system model. Even though the use of this model provided a sufficient control, use of an adaptive model which adjusts the model parameters in

accordance with the change in their respective system parameters, will improve the performance of the predictive controller.

BIBLIOGRAPHY

1. Billingsley, J., J. F. Coales. Simple predictive controller for higher order systems. Institute of Electrical Engineers Proceedings. October 1968.

2. Chestnut, H., W. E. Sollecito, P. H. Troutman. Predictive control system application. American Institute of Electrical Engineers Transaction, Part II, Application and Industry. July 1961.

3. Fallside, F., N. Thedchanamoorthy. Predictive control using an adaptive fast model. Institute of Electrical Engineers Proceedings. November 1967.

4. Gibbons, J. F. Semiconductor electronics. McGraw-Hill Book Company. 1966.

5. Gourishankar, V. Electromechanical energy conversion. International Textbook Company. September 1965.

6. Philbrick/Nexus Research. Dedham, Mass. Application Manual-Computing Amplifiers. February 1968.

7. Pontryagin, L. S., V. G. Boltyanskii, R. V. Gamkrelidze and I. F. Mischenko. The mathematical theory of optimal processes. Wiley. 1962.

8. Rae, W. G. Fast model search control systems. International Journal of Control. October 1967.

APPENDICES

APPENDIX A

THE DIFFERENTIATOR

The derivative of the output voltage of the d-c generating system was obtained using the elementary rules of analog differentiation, followed by some modifications necessary to make the differentiator dynamically stable. Figure A-1 shows the analog diagram of the differentiator, using an operational amplifier.

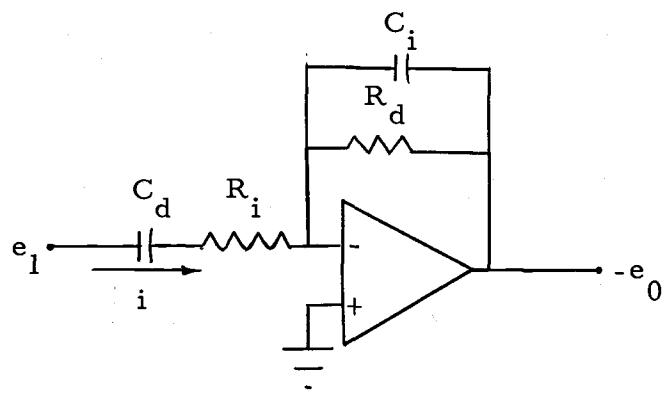

Figure A-1. The differentiator.

The input capacitor, C_d, and the feedback resistor, R_d, are the prime factors in the differentiation process, while the input resistor, R_i, and the feedback capacitor, C_i, are also necessary to attenuate the high frequency noise, generated by the differentiation process (6). A frequency, ω_c, is chosen such that for frequencies below that, the differentiation process is carried on, and for frequencies greater than ω_c, the signal is integrated in order to attenuate the undesired high frequency noise. ω_c is chosen higher than the highest frequency

component of the input signal to the differentiator, so that the high frequency noise attenuation will not affect the output-rate of the d-c generating system.

From the above introduction it can be seen that the designed differentiator is actually a bandpass filter about ω_c.

In Figure A-1, the output voltage e_0 can be obtained in terms of e_1 as follows:

$$I(s) = \frac{E_1(s)}{R_i + \frac{1}{SC_d}} = \frac{SE_1(s)C_d}{1 + SR_iC_d} \qquad (A\text{-}1)$$

Where $E_1(s)$ and $I(s)$ are the Laplace Transforms of the time domain parameters $e_1(t)$ and $i(t)$, respectively. Laplace Transform of the output of the differentiator is

$$E_0(s) = - I(s) \frac{R_d/SC_i}{R_d + \frac{1}{SC_i}} \qquad (A\text{-}2)$$

Substituting Equation (a-1) into (A-2), it yields:

$$E_0(s) = - \frac{R_dC_d}{(1 + sT_c)^2} SE_1(s) \qquad (A\text{-}3)$$

where

$$T_c = R_dC_i = R_iC_d = \frac{2\pi}{\omega_c}$$

Taking the inverse Laplace Transform of Equation (A-3), the time domain expression for the output of the differentiator will result:

$$e_0(t) = -\frac{R_d C_d p}{(1 + T_c p)^2} e_1(t) \qquad \text{(A-4)}$$

where $p = d/dt$.

From Equation (A-4) it is clear that for low frequencies the output is differentiated, and for high frequencies the output signal is integrated, in order to attenuate the high frequency noise.

The anticipated frequency of the input signal to the differentiator was between 60-80 radians/second. The feedback resistor $R_d = 100k\Omega$ was fixed in the operational amplifier. Other parameters were chosen as follows, to meet the frequency and gain requirements.

C_d = 10 microfarads

R_i = 7.5 kilo ohms

C_i = 0.75 microfarads

With these chosen parameters

T_c = 0.075 seconds

and

$$\omega_c = 2\pi/0.075 = 83.7$$

This meets the requirement that $\omega_c > \omega$, where ω is the highest frequency component of the input signal to the differentiator.

The differentiator was used as a part of the control system, and its response is shown among the experimental results presented in part V of this thesis.

APPENDIX B

THE CURRENT CONTROLLER

The purpose of the current controller is to produce a desired change in the exciter field current for some change in its input voltage V_b. A simple transistor current amplifier is used for this purpose. The amplifier is connected in series with exciter field winding, as shown in Figure B-1, so that the exciter field current, i_{fe}, is the same as the amplifier collector current.

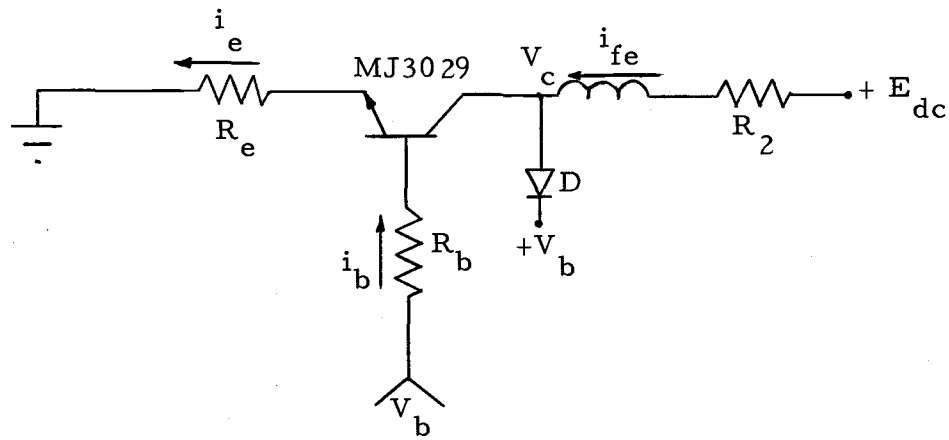

Figure B-1. The field current controller.

Before the transistor goes into saturation, its input current, i_b, is proportional to the emitter current, i_e,

$$i_b = \frac{V_b}{R_b} = \frac{i_e}{\beta} \qquad \text{(B-1)}$$

where β is the transistor current gain. Since $i_e \approx i_{fe}$, from Equation (B-1):

$$i_{fe} = \frac{\beta}{R_b} V_b \qquad (B-2)$$

which shows the controllability of i_{fe} through control of V_b.

Diode D is used for safety purposes, so that the collector voltage V_c will not exceed its limit, V_D, which depends on the type of transistor.

Resistors, R_b and R_e, were chosen such that, V_b and C, which were respectively determined and accepted by the computer, would stay in the computer voltage range (-10 to 10 volts). The chosen values were as follows:

$$R_b = 2.2 \text{ kilo ohms}$$

$$R_e = 4.6 \text{ ohms}$$

A calibration curve of input A versus the scaled system output, C, was obtained as shown in Figure B-2. This curve was used to assure that the values chosen for V_b would not saturate the transistor, and also, that for the chosen values of V, the scaled output would not overload the computer.

In Figure B-2 the slope of the linear approximation of the curve is the overall gain of the d-c generating system. The linear approximation of the curve is extended to find the approximate offset from the origin. This offset is used as a part of the input to the fast model (see Appendix D, Figure D-2).

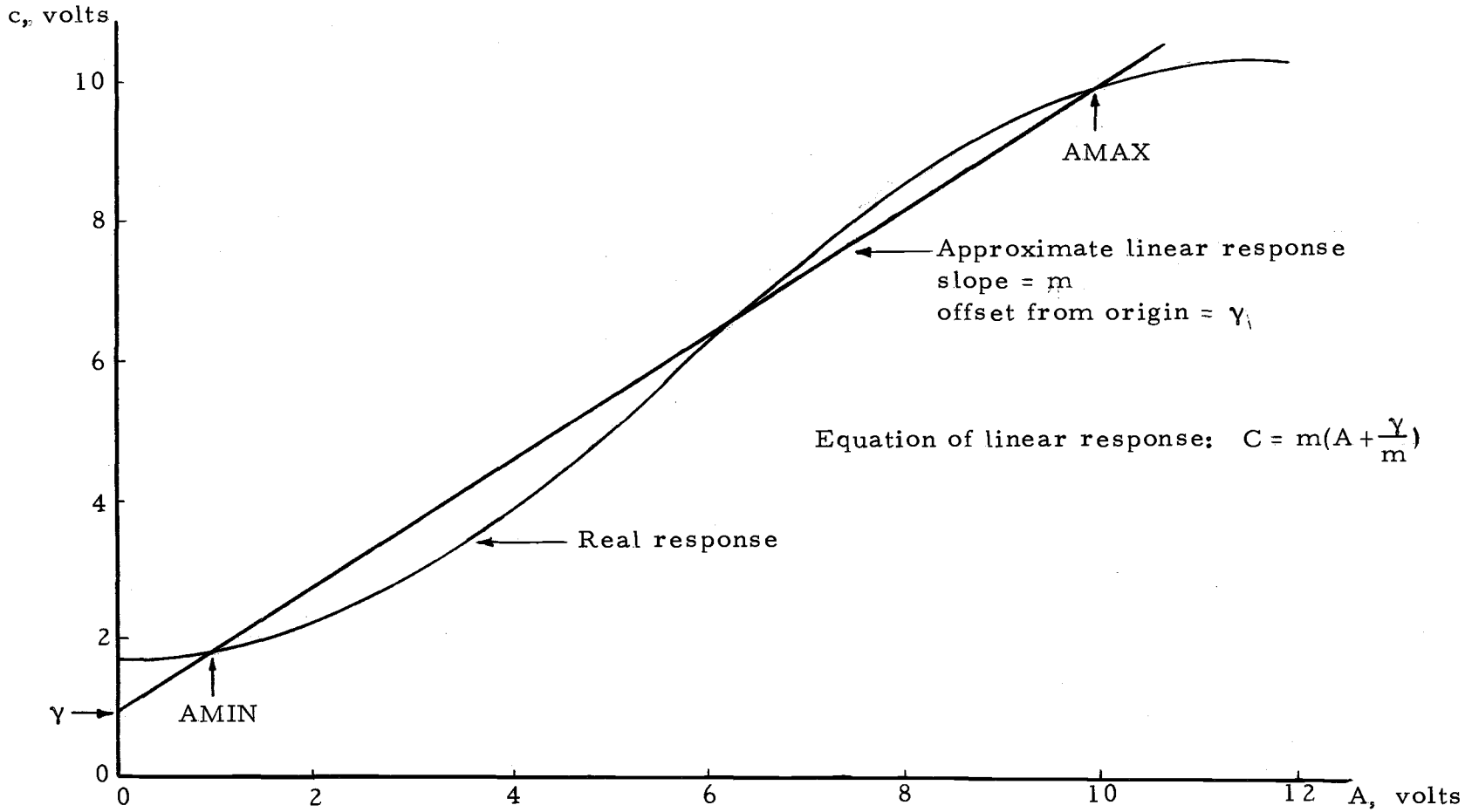

Figure B-2. Calibration curve of input, A, versus output, C.

APPENDIX C

GENERATOR SPECIFICATIONS

Exciter: General Electric DC-generator

Voltage rating = 240 volts

R_{fe} = 195 ohms

L_{fe} = 125 henries

R_{ae} = 0.3 ohm

$L_{ae} \tilde{=}$ 10 millihenries

Generator: General Electric DC-generator

Voltage rating = 240 volts

R_{fg} = 690 ohms

L_{fg} = 147 henries

R_{ag} = 2.4 ohms

$L_{ag} \tilde{=}$ 10 millihenries

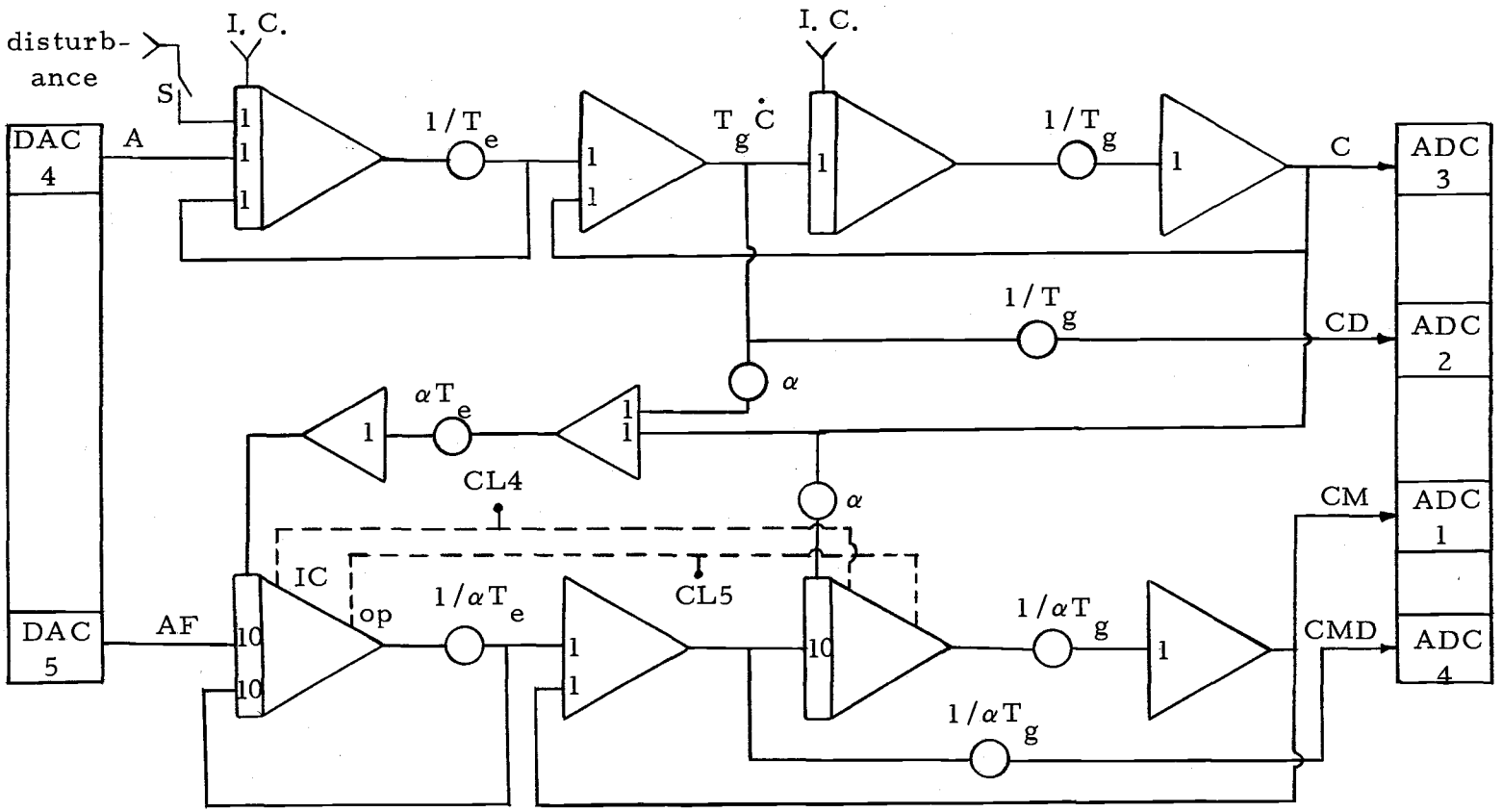

Figure D-1. Analog simulation diagram of the controlled system in connection with its fast-time scale model. In this simulation model time scale is 10.

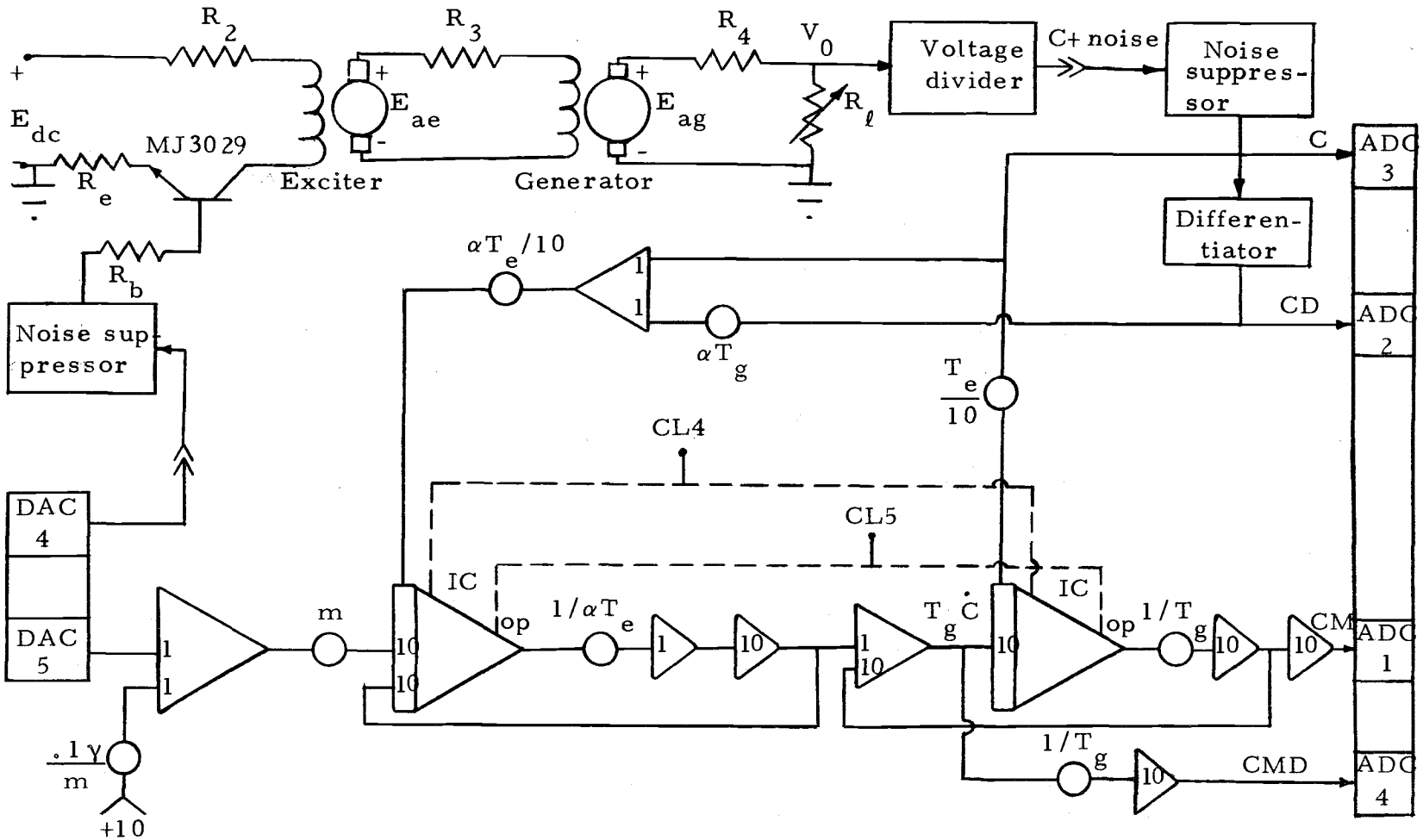

Figure D-2. Analog simulation diagram of the fast model, connected to the controlled system. In this diagram model time scale is 100, and the model is magnitude scaled by 10.